Impulse framework for unsteady flows reveals superdiffusive bed load transport

Colin B. Phillips,[1] Raleigh L. Martin,[1] and Douglas J. Jerolmack[1]

Received 28 January 2013; revised 1 March 2013; accepted 4 March 2013; published 11 April 2013.

[1] Sediment transport is an intrinsically stochastic process, and measurement of bed load in the environment is further complicated by the unsteady nature of river flooding. Here we present a methodology for analyzing sediment tracer data with unsteady forcing. We define a dimensionless impulse by integrating the cumulative excess shear velocity for the duration of measurement, normalized by grain size. We analyze the dispersion of a plume of cobble tracers in a very flashy stream over two years. The mean and variance of transport distance collapse onto well-defined linear and power-law relations, respectively, when plotted against cumulative dimensionless impulse. Data suggest that the asymptotic limit of bed load tracer dispersion is superdiffusive, in line with a broad class of geophysical flows exhibiting strong directional asymmetry (advection), thin-tailed step lengths and heavy-tailed waiting times. The impulse framework justifies the use of quasi-steady flow approximations for long-term river evolution modeling.
Citation: Phillips, C. B., R. L. Martin, and D. J. Jerolmack (2013), Impulse framework for unsteady flows reveals superdiffusive bed load transport, *Geophys. Res. Lett.*, *40*, 1328–1333, doi:10.1002/grl.50323.

1. Introduction

[2] Coarse-grained river cobbles spend only a small fraction of their time in motion. Even when fluid stress is above the threshold of motion, a cobble is predominantly at rest under most bed load transport conditions. Sediment transport at the particle scale can be described as a series of steps and rests, whose respective lengths and durations may be determined by theory or experiment [*Einstein*, 1937]. Recent particle tracking experiments along these lines have suggested that bed load particles are separated into mobile and immobile populations, with an exchange rate among them determined by transition probabilities [*Ancey et al*., 2008]. A momentum balance approach at the grain and bulk scales has been utilized to derive relations between fluid shear velocity and particle step length, particle velocity, and number of mobile particles [*Charru et al*., 2004; *Lajeunesse et al*., 2010]. Video particle tracking in both the field and the laboratory has allowed the determination of tracer diffusion regimes [*Nikora et al*., 2002] and the physical processes responsible for particle dispersion [*Martin et al*., 2012]. Diffusive regimes are commonly determined through scaling of the diffusion exponent (γ), which relates the variance in particle displacement (σ^2) to time (t) such that $\sigma^2 \sim t^\gamma$ [e.g., *Metzler and Klafter*, 2000]. For $\gamma = 1$, diffusion is normal; for all other values of γ, diffusion is anomalous where for $\gamma < 1$ processes are subdiffusive; and for $\gamma > 1$ processes are superdiffusive [e.g., *Metzler and Klafter*, 2000]. *Nikora et al*. [2002] identified three bed load scaling regimes: the local range of individual ballistic particle trajectories, an intermediate range consisting of many ballistic particle trajectories, and a global range consisting of many intermediate particle trajectories. *Martin et al*. [2012] showed that dispersion in the local regime is ballistic due to correlated particle motions and that heavy-tailed particle waiting times caused by burial and scour under low-stage transport could possibly explain anomalous diffusion in the global regime. In the global range both subdiffusion and superdiffusion have been reported [*Nikora et al*., 2002; *Bradley et al*., 2010].

[3] Due to the limited length of laboratory experiments and the demand to understand bed load in natural systems, particle tracking in the field has become an attractive approach. Sediment tagged with Radio Frequency Identification Passive Integrated Transponders (RFID PIT) allows the tracking of individual particles at long timescales. This tracking method has been used in rivers to determine particle vertical mixing rates, bed and bed form mobility, virtual velocity, sand and gravel dispersion, and gravel step lengths and rest durations as well as the effects of alluviation and topography on these parameters [e.g., *Habersack*, 2001; *Nikora et al*., 2002; *Ferguson et al*., 2002; *Haschenburger and Wilcock*, 2003; *Bradley et al*., 2010; Bradley and Tucker, 2012; *Hodge et al*., 2011; *Hassan et al*., 2013]. At the flood and multi-flood scale, sediment tracer data represent a cumulative measure of individual particle path lengths (global regime of *Nikora et al*. [2002]). Given the difficulties of unsteady forcing in a single flood and a series of floods (Figure 1a), a framework incorporating an unsteady flow is essential. Inspired by the impulse framework introduced by *Diplas et al*. [2008] to account for turbulence, we develop a nondimensional impulse to characterize macroscopic variations in fluid stress due to an unsteady hydrograph. We then apply this framework to a new bed load tracer study and demonstrate that the data collapse onto physically meaningful curves of travel distance and dispersion.

2. Impulse Framework

[4] Particles resting on a stream bed require a stress above a threshold value to begin moving [e.g., *Buffington and Montgomery*, 1997]. Laboratory experiments have established that once a sediment particle is pried free of the bed it exhibits a velocity and step length linearly proportional to excess shear

[1]Department of Earth and Environmental Science, University of Pennsylvania, Philadephia, Pennsylvania, 19104, USA.

Corresponding author: C. B. Phillips, Department of Earth and Environmental Science, University of Pennsylvania, Philadephia, Pennsylvania, 19104, USA. (colinp@sas.upenn.edu)

0094-8276/13/10.1002/grl.50323

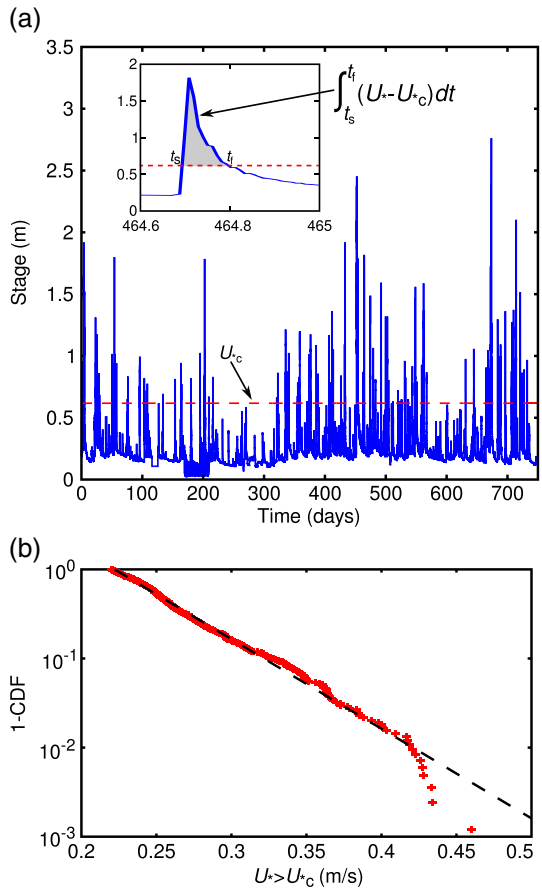

Figure 1. (a) Hydrograph in stage (m) for the Mameyes River for the duration of the field study. The dashed red line represents the empirically determined threshold of motion $U_{*c} = 0.22$ m/s (Shields stress of 0.023). The inset is of a single flood with the shaded region representing the flood impulse (see text section 2). (b) Distribution of shear velocity greater than the critical shear velocity.

velocity ($U_* - U_{*c}$), where U_* [m/s] is the shear velocity and U_{*c} is the threshold shear velocity for initiation of motion [*Francis*, 1973; *Fernandez Luque and Van Beek*, 1976; *Lajeunesse et al.*, 2010; see Table 3 in *Martin et al.*, 2012]. The duration of motion for a particle during a flood is unknown; however, it seems clear based on the arguments above that particle displacement should be proportional to the product of (i) the velocity of the particle when in motion and (ii) the duration of flow in excess of the threshold of motion. This can be encoded in a cumulative dimensionless impulse, I_*, that is a kind of transport length:

$$I_* = \int_{t_s}^{t_f} (U_* - U_{*c})dt/D_{50}, \quad U_* > U_{*c}, \tag{1}$$

where t_s and t_f are the starting and finishing times of the considered hydrograph record, and D_{50} is the median grain size of the stream. We consider only flows in excess of U_{*c} in (1), which truncates the frequency-magnitude distribution of U_* by excluding all subthreshold flows (which are irrelevant for transport) present in the hydrograph(Figure 1b). This removes the effect of flood recurrence intervals—which are determined by regional climate—and only considers sediment transport as a function of excess momentum imparted on the grains. Our treatment assumes a constant U_{*c} and thus ignores potential variations (temporal and spatial) in the threshold of motion; however, these could be incorporated in the future. For our field study U_{*c} is empirically determined from tracer particles (see section 3), but a first approximation could be derived from the Shields curve. In the following paragraphs we demonstrate the utility of this dimensionless impulse framework with a field dataset of tracer particles.

3. Field Study

[5] The field tracer experiment was performed in the Mameyes River in the Luquillo Critical Zone Observatory in North East Puerto Rico. The Mameyes River is nestled in the heart of the Luquillo Mountains, which have a strong orographic effect resulting in greater than 4000 mm/yr of precipitation. Precipitation occurs as short-duration, high-magnitude events which result in frequent flash flooding [*Schellekens et al.*, 2004]. The study reach is a cobble-bedded, 1.2 km stretch of the Mameyes River just downstream of its exit from the mountains; it exhibits nearly uniform width (20 m), minimal meandering, and a slope of $S = 7.8 \times 10^{-3}$. The slope represents a linear regression of the channel longitudinal profile extracted from a lidar digital elevation model (DEM) (1 m horizontal and vertical resolution). Stage (h) was recorded every 5 min at the site for 40 days by an In-Situ Level Troll 500 and correlated to measurements from a U.S. Geological Survey (USGS) gage 3.5 km upstream (15 min resolution) to obtain a stage record for the duration of study.

[6] For the study reach $U_* = (ghS)^{1/2}$ was estimated assuming steady and uniform flow, where g is acceleration due to gravity; Shields stress, $\tau_* = U_*^2/(RgD_{50})$, was also estimated for comparison to other studies, where $R = 1.65$ is the submerged specific gravity of the tracers. We do not attempt to justify the normal flow approximation physically, although channel geometry is remarkably consistent along the study reach; rather, it is a convenient simplification that will be assessed *a posteriori*. We computed the I_* (1) for each flood, over the 2 year study period (Figure 1a). We also examined the frequency-magnitude distribution of shear velocity values in excess of critical ($U_* > U_{*c}$), finding an exponential distribution (Figure 1b); a similar result was obtained when all 20 years of stage data were used. This implies that there is a well-defined average or "characteristic" shear velocity associated with floods; we return to the implications of this finding below.

[7] RFID PIT tags with unique numbers were installed in 300 cobbles in two separate populations of 150 cobbles placed in the stream, in a 20 × 20 m grid with 1 m spacing spanning the channel, in the summers of 2010 and 2011. Tracer particle positions were surveyed two, three, and one time(s) in the summers of 2010, 2011, and 2012, respectively (Figures 2a–2c respectively). Positions were transformed from Cartesian coordinates to a stream-wise normal coordinate system following a methodology similar to *Legleiter and Kyriakidis* [2007]. Total tracer recovery percentages for all six surveys for population one were 62%, 92.5%, 86.6%, 88%, 86.6%, and 93%. Tracer recovery for all three surveys for population two were 100%, 99%, and 94.6%. The low recovery of the initial survey of population one was due to limited sampling time between flooding events. Tracer particle populations were selected from the stream bed to have narrow grain size distributions in order to promote equal mobility [*Wiberg and Smith*, 1987] among the tracers (Figure 2a inset).

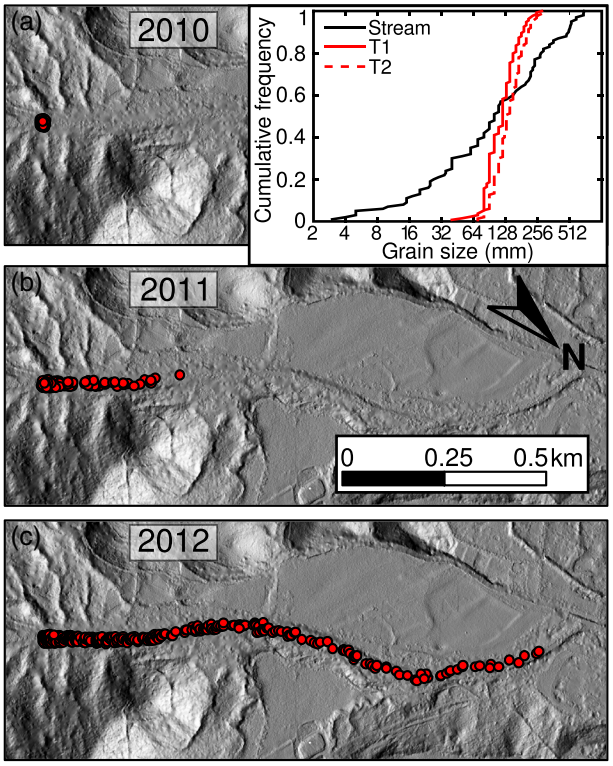

Figure 2. (a) Location of tracer particle initial placement on lidar DEM of the study area in May of 2010. The inset shows the cumulative grain size distributions for the stream (black line), and tracer population one and two (red and dashed red lines respectively). (b) Location of tracer particles in summer 2011. (c) Location of tracer particles in summer 2012.

The median grain size values for the stream and tracer populations one and two were 12, 12, and 13 cm, respectively. The stream D_{50} represents the average of three pebble counts [*Wolman*, 1954]. During transport, tracers were fully submerged (average $h/D_{50} = 7.0$). Tracer particles were located with two wands manufactured by Oregon RFID with maximum detection radii of 50 cm and 20 cm. Survey and detection error were set at 45 cm and 1 m for the small and large wands, respectively, which is 1.5 times the calculated combined survey and detection error. RFID tags are detectable at burial depths up to 50 cm and 10–20 cm, depending on tag orientation, for the large and small wands, respectively.

4. Results and Analysis

[8] Several individual floods were surveyed in the summers of 2010 and 2011 and were used to calculate the distributions of particle travel length and also the fraction of mobile particles, f. For single floods each tracer's transport distance (X_i) was normalized by its median diameter (D_i) (Figure 3a), such that X_i/D_i represents the dimensionless transport distance of an individual tracer. Displacement distances of tracers for each flood are well characterized by an exponential distribution (Figure 3a). Typical distances of individual tracers were a few meters for a given flood, implying very intermittent (rather than continuous) transport.

[9] We anticipate a linear relation between the peak flood Shields stress and the mobile fraction (i.e., $f \sim \tau_*$) based on momentum balance [*Lajeunesse et al.*, 2010] and determined

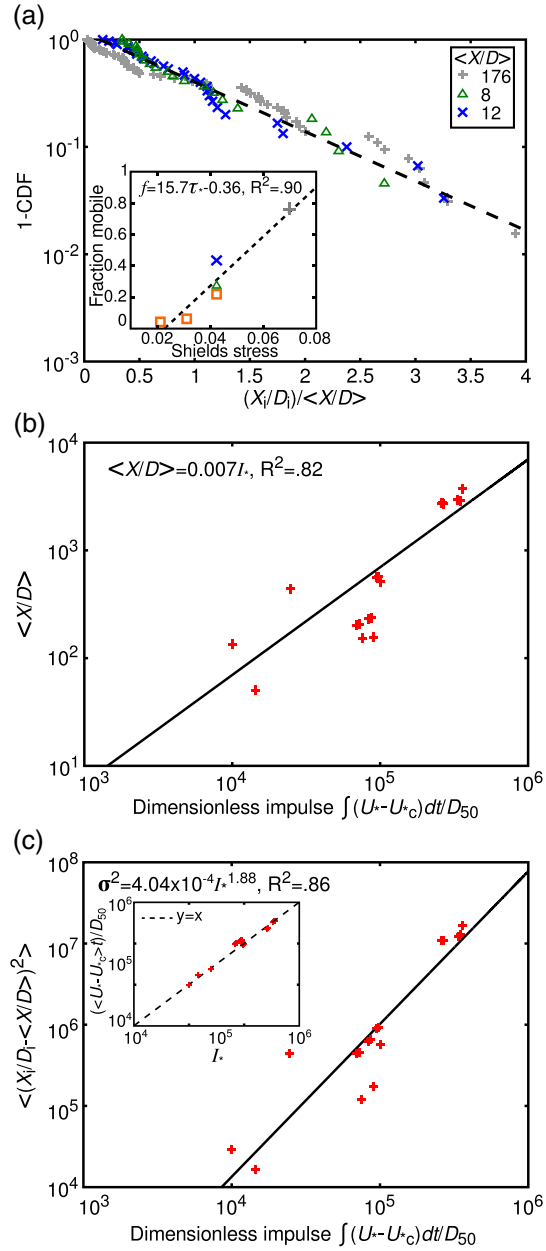

Figure 3. (a) Dimensionless step length distributions for individual floods normalized by the mean ($<X/D>$) step length for each flood. Dimensionless mean step lengths for each flood are labeled in the legend. The dashed black line represents an exponential distribution. The inset represents the fraction of tracers that moved against the peak Shields stress for each flood. Symbols and colors correspond to the same datasets for both the inset and Figure 3a. (b) Scaling of the mean dimensionless tracer transport distance against dimensionless impulse; the solid black line represents a linear fit through the origin. (c). Scaling of the variance with dimensionless impulse; the solid black line represents the best-fit relationship. The inset shows the equivalence between the dimensionless impulse, and the dimensionless time similar to *Nikora et al.* [2002].

U_{*c} from the intercept of this fit (Figure 3a inset). We estimated $\tau_{*c} = 0.023$, or $U_{*c} = 0.22$ m/s, for the tracer D_{50}. Note that $f < 1$ for all floods, implying that continuous

bed load transport did not occur for even the largest events; this is consistent with the inference of intermittent transport from travel distances.

[10] We determined scaling of the mean ($<X/D>$) and variance ($\sigma^2 = <(X_i/D_i - <X/D>)^2>$) of dimensionless tracer transport distances as a function of I_*. Following the reasoning of section 2 we anticipate a linear relationship between I_* and $<X/D>$. Here the $<>$ symbols represent the ensemble average over all particles. When interpreting fitting exponents of the mean and variance, we make the assumption that tracer displacement has reached the asymptotic limit; i.e., transport is not in a transient regime. Due to the limited number of sampling intervals, we utilized all permutations of tracer surveys. Values for $<X/D>$ collapse onto a reasonably linear relation when plotted against I_* (Figure 3b). The fitted equation in Figure 3b represents the ratio of the mean values of I_* and $<X/D>$. We also find data collapse of the variance onto a power-law relationship when plotted against I_* (Figure 3c). There is no systematic trend for $<X/D>$ and the variance when plotted against real (clock) time. We note that the values of I_* in Figures 3b and 3c are sensitive to the value of U_{*c}, but that the form of the scaling relationships are robust.

[11] The linear form of Figure 3b implies a constant mean tracer virtual velocity. This suggests that at long timescales cumulative impulse is proportional to (and dominated by) the duration of time above threshold, i.e., $I_* \sim t$, where t represents the total time above the threshold of motion. Indeed, we recover nearly identical scaling (as in Figures 3b and 3c) when the I_* is replaced by $< U_* - U_{*c} > t / D_{50}$, because (see Figure 3c inset) $I_* \approx \langle U_* - U_{*c} \rangle t/D_{50}$ for our study system, where $< U_* - U_{*c} >$ is the average value for the distribution of $U_* > U_{*c}$ (Figure 1b). The parameter $< U_* - U_{*c} > t / D_{50}$ is similar to the dimensionless time used by *Nikora et al.* [2002] for investigating bed load diffusion scaling. We can now interpret the mean square displacement as representing dispersion of tracers as a function of transport time; the scaling exponent, $\gamma = 1.88$, ($\sigma^2 \sim t^\gamma$), indicates superdiffusion.

[12] The tracer waiting time distribution is not directly measurable, however, there is an expectation based on experiments by *Martin et al.* [2012] for heavy-tailed waiting times. In the case of symmetric random walks, thin-tailed step lengths and heavy-tailed waiting times produce subdiffusive behavior [e.g., *Weeks et al.*, 1996; *Metzler and Klafter*, 2000]. However, in the presence of a strong asymmetry (drift), the same distributions can produce superdiffusive scaling [*Weeks et al.*, 1996]. In the case of a river where steps occur in only one direction—i.e., downstream—long waiting times would appear as Levy flights in the upstream direction when viewed from a Lagrangian reference frame centered on $<X/D>$ [*Weeks et al.*, 1996]. Indeed, our $<X/D>$ measurements support a constant unidirectional drift (Figure 3b). Using the analytical framework for asymmetric random walks [*Weeks et al.*, 1996; *Weeks and Swinney*, 1998] and the knowledge that particle step lengths are thin tailed (exponential), we infer that cobbles exhibit a power-law waiting time distribution with an exponent $\nu = 4 - \gamma = 2.12$ for the probability density function. It should be noted that this is the inferred waiting time distribution during flows above threshold, and that the time below threshold is not considered.

5. Discussion and Summary

[13] The novelty and utility of I_* is that it allows the coupling of hydrological and sediment tracer data well beyond the single-flood scale, in a physically based manner. For channels where the distribution of $U_* > U_{*c}$ is thin tailed, I_* can also be viewed as a dimensionless time following the reasoning of *Nikora et al.* [2002]. An assumption in this study is that U_{*c} is constant, which is not valid in some situations [*Kirchner et al.*, 1990; *Charru et al.*, 2004; *Marquis and Roy*, 2012]. This assumption is made out of necessity as there is currently no feasible manner in which to determine U_{*c} for each flood. However, the collapse of the mean and variance of tracer displacement data suggests that the range of values for U_{*c} cannot be large in this reach during the study period. Our tracer recovery rates (excluding the first flood) were consistently higher than other similar studies [*Ferguson et al.*, 2002; *Haschenburger*, 2011a; *Liébault et al.*, 2012]. However, there is a potential for the scaling exponents γ and ν to be biased by unrecovered tracers, which would likely have traveled the farthest and hence have had significant influence on calculated means and variances. It is possible that tracers were destroyed or buried beyond the detection limit, though the latter is unlikely as similar studies reported fairly shallow burial depths for a large range of conditions [*Haschenburger*, 2011b; *Houbrechts et al.*, 2012]. However, the missing tracers are likely to affect each survey in a similar manner, in that increasing $<X/D>$ and σ^2 would simply rescale the linear and power law relationships for $<X/D>$ and σ^2, respectively. We thus treat our scaling exponents as estimates of their actual values. In the experiments of *Martin et al.* [2012] the heavy-tailed waiting time distribution was the result of the time it took to scour down to the depth of the buried tracer. If the inferred heavy-tailed distribution of tracer waiting times in this study is accurate, this lends further support to the mobile and immobile partition [*Ancey et al.*, 2008] of sediment tracers, with a residence time in the immobile phase that is controlled by erosion and deposition of the bed [*Martin et al.*, 2012].

[14] The similarity of cumulative impulse and $< U_* - U_{*c} > t$ implies that unsteadiness of the hydrograph may be further simplified through use of an intermittency factor $I = t / T$, where T is the total duration of elapsed (clock) time. The time-integrated hydrograph then reduces to a form $I < U_* - U_{*c} > T$, which is precisely the treatment used in long-term modeling of river profiles [e.g., *Paola et al.*, 1992; *Parker et al.*, 1998]. For floods exceeding critical shear velocity in our period of study, $<U_*> = 0.27$ m/s ($<\tau_*> = 0.032$) and the ratio of $< \tau_* > / \tau_{*c} = 1.39$; this is close to the theoretically predicted and measured bankfull flow values for bed load–dominated alluvial streams at equilibrium, τ_*/τ_{*c} of 1.2 and ~1.4, respectively [*Parker*, 1978; *Paola et al.*, 1992; *Parker et al.*, 1998]. Despite the (perhaps fortuitous) validation of landscape modeling assumptions made by *Paola et al.* [1992], this simplification is only valid at timescales sufficiently longer than the recurrence interval of floods and requires that the distribution of $U_* > U_{*c}$ is well behaved (i.e., that it is thin tailed). For the Mameyes River, the short recurrence interval of floods exceeding critical shear velocity (~5 days) hastens this convergence. Nonetheless, it is remarkable that the complex hydrograph (Figure 1a) may be reduced to an average stress with an intermittency factor and still describe the mean tracer displacement.

[15] Anomalous diffusion of sediment tracers in the global regime of *Nikora et al*. [2002] has been suggested by modeling [*Ganti et al*., 2010] and field studies [*Bradley et al*., 2010; *Liébault et al*., 2012], though usually due to heavy-tailed step lengths. The existence of heavy-tailed step lengths in natural tracer studies is still a matter of debate [*Hassan et al*., 2013]. In this tracer study we do not observe heavy-tailed step lengths. It is possible that our selection of a narrow tracer grain-size distribution precludes the emergence of heavy-tailed step lengths observed in experiments by *Hill et al*. [2010]. This interpretation is supported by the experimental results of *Roseberry et al*. [2012], which show thin-tailed step length distributions for nearly unimodal sediment under steady flow. Our inferred heavy-tailed waiting times emerge only when considering flows above the threshold of motion and thus are unrelated to flood recurrence [*Zhang et al*., 2012]. *Nikora et al*. [2002] suggested that heavy-tailed waiting times would lead to subdiffusion in the global regime; however, because sediment tracers undergo asymmetric random walks, the heavy-tailed waiting times produce superdiffusion. *Zhang et al*. [2012] point out that at the longest timescales, one should eventually observe normal diffusion because particle waiting times will not be infinitely long; however, in practice the waiting times of field tracers may be sufficiently long that this "normal" scaling is never observed. At present, we have no basis for estimating the maximum particle waiting time in a river. An additional caveat is that our particles may not have sampled sufficient space and time to reach the asymptotic scaling limit, and so caution should be applied when inferring scaling exponents from these data. If results are taken at face value, however, they suggest that bed load tracers behave similarly to tracers in other geophysical flows [*Weeks et al*., 1996] and also to charge carriers in amorphous materials [*Scher and Montroll*, 1975], where heterogeneity leads to long particle trapping times in the presence of strong drift. Furthermore, the dimensionless impulse could act as a catalyst for synthesizing existing bed load tracer datasets. Should the results of our study be borne out in other rivers, we might be emboldened to extrapolate bed load dynamics beyond tracer observations using existing hydrologic gage data. If the characteristic flood magnitude and intermittency of a given river could be assumed reasonably constant, one could even estimate bed load travel distances over geologic timescales. This could provide one way to estimate the residence time of cobbles in a river, if their provenance was known.

[16] **Acknowledgments.** We thank J. Singh, K. Litwin, D. Miller, R. Glade, and J. Evaristo for outstanding field assistance. We thank D. N. Bradley for assistance concerning tracer tracking equipment. We thank C. Ancey and an anonymous reviewer for thoughtful reviews. We gratefully acknowledge the Luquillo Critical Zone Observatory (NSF EAR 0722476) and the University of Pennsylvania Benjamin Franklin Fellowship program for logistical and financial support.

References

Ancey, C., A. C. Davison, T. Bohm, M. Jodeau, and P. Frey (2008), Entrainment and motion of coarse particles in a shallow water stream down a steep slope, *J. Fluid Mech.*, *595*, 83–114, doi:10.1017/S0022112007008774.

Bradley, D. N., G. E. Tucker, and D. A. Benson (2010), Fractional dispersion in a sand bed river, *J. Geophys. Res.*, *115*, 20, doi:10.1029/2009JF001268.

Bradley, D. N., and G. E. Tucker (2012), Measuring gravel transport and dispersion in a mountain river using passive radio tracers, *Earth Surf. Process. Landforms*, *37*(10), 1034–1045, doi:10.1002/esp.3223.

Buffington, J. M., and D. R. Montgomery (1997), A systematic analysis ofeight decades of incipient motion studies, with special reference to gravel-bedded rivers, *Water Resour. Res.*, *33*(8), 1993–2029, doi:10.1029/96WR03190.

Charru, F., H. Mouilleron, and O. Eiff (2004), Erosion and deposition ofparticles on a bed sheared by a viscous flow, *J. Fluid Mech.*, *519*, 55–80, doi:10.1017/S0022112004001028.

Diplas, P., C. L. Dancey, A. O. Celik, M. Valyrakis, K. Greer, and T. Akar (2008), The role of impulse on the initiation of particle movement under turbulent flow conditions, *Science*, *322*(5902), 717–720, doi:10.1126/science.1158954.

Einstein, H. A. (1937), Bed load transport as a probability problem, PhD thesis, Res. Inst. of Hydraul. Eng., Eidgenossische Tech. Hochschule, Zurich, Switzerland.

Ferguson, R. I., D. J. Bloomer, T. B. Hoey, and A. Werritty (2002), Mobility of river tracer pebbles over different timescales, *Water Resour. Res.*, *38*(5), 1045, doi:10.1029/2001WR000254.

Fernandez Luque, R., and R. Van Beek (1976), Erosion and transport of bed-load sediment, *J. Hydraul. Res.*, *14*, 127–144.

Francis, J. R. D. (1973), Experiments on the motion of solitary grains along the bed of a water-stream, *Proc. R. Soc. London, Ser. A.*, *332*(1591), 443–471.

Ganti, V., M. M. Meerschaert, E. Foufoula-Georgiou, E. Viparelli, and G. Parker (2010), Normal and anomalous diffusion of gravel tracer particles in rivers, *J. Geophys. Res.*, *115*, 12, doi:10.1029/2008JF001222.

Habersack, H. M. (2001), Radio-tracking gravel particles in a large braided river in New Zealand: A field test of the stochastic theory of bed load transport proposed by Einstein, *Hydrol. Process.*, *15*(3), 377–391, doi:10.1002/hyp.147.

Haschenburger, J. K., and P. R. Wilcock (2003), Partial transport in a natural gravel bed channel, *Water Resour. Res.*, *39*, 9, doi:10.1029/2002WR001532.

Haschenburger, J. K. (2011a), The rate of fluvial gravel dispersion, *Geophys. Res. Lett.*, *38*(24), L24403, doi:10.1029/2011GL049928.

Haschenburger, J. K. (2011b), Vertical mixing of gravel over a long flood series, *Earth Surf. Process. Landforms*, *36*(8), 1044–1058, doi:10.1002/esp.2130.

Hassan, M. A., H. Voepel, R. Schumer, G. Parker, and L. Fraccarollo (2013), Displacement characteristics of coarse fluvial bed sediment, *J. Geophys. Res.*, *118*, doi:10.1029/2012JF002374.

Hill, K. M., L. DellAngelo, and M. M. Meerschaert (2010), Heavy-tailed travel distance in gravel bed transport: An exploratory enquiry, *J. Geophys. Res.*, *115*, F00A14, doi:10.1029/2009JF001276.

Hodge, R. A., T. B. Hoey, and L. S. Sklar (2011.), Bedload transport inbedrock rivers: The role of sediment cover in grain entrainment, translation and deposition, *J. Geophys. Res.*, doi:10.1029/2011JF002032., in press.

Houbrechts, G., J. Van Campenhout, Y. Levecq, E. Hallot, A. Peeters, and F. Petit (2012), Comparison of methods for quantifying active layer dynamics and bedload discharge in armoured gravel-bed rivers, *Earth Surf. Process. Landforms*, *37*(14), 1501–1517, doi:10.1002/esp.3258.

Kirchner, J. W., W. E. Dietrich, F. Iseya, and H. Ikeda (1990), The variability of critical shear stress, friction angle, and grain protrusion in water worked sediments, *Sedimentology*, *37*, 647–672.

Lajeunesse, E., L. Malverti, and F. Charru (2010), Bed load transport in turbulent flow at the grain scale: Experiments and modeling, *J. Geophys. Res.*, *115*, 16, doi:10.1029/2009JF001628.

Legleiter, C., and P. Kyriakidis (2007), Forward and inverse transformations between Cartesian and channel-fitted coordinate systems for meandering rivers, *Math. Geol.*, *38*(8), 927–958, doi:10.1007/s11004-006-9056-6.

Liébault, F., H. Bellot, M. Chapuis, S. Klotz, and M. Deschâtres (2012), Bedload tracing in a high-sediment-load mountain stream, *Earth Surf. Process. Landforms*, *37*(4), 385–399, doi:10.1002/esp.2245.

Marquis, G. A., and A. G. Roy (2012), Using multiple bed load measurements: Toward the identification of bed dilation and contraction in gravel-bed rivers, *J. Geophys. Res.*, *117*(F1), F01014, doi:10.1029/2011JF002120.

Martin, R. L., D. J. Jerolmack, and R. Schumer (2012), The physical basis for anomalous diffusion in bed load transport, *J. Geophys. Res.*, *117*(F1), F01018, doi:10.1029/2011JF002075.

Metzler, R., and J. Klafter (2000), The random walk's guide to anomalous diffusion: A fractional dynamics approach, *Phy. Rep.*, *339*(1), 1–77, doi:10.1016/S0370-1573(00)00070-3.

Nikora, V., H. Habersack, T. Huber, and I. McEwan (2002), On bed particle diffusion in gravel bed flows under weak bed load transport, *Water Resour. Res.*, *38*, 9, doi:10.1029/2001WR000513.

Paola, C., P. L. Heller, and C. L. Angevine (1992), The large-scale dynamics of grain-size variation in alluvial basins: 1. Theory, *Basin Res.*, *4*, 73–90.

Parker, G. (1978), Self-formed straight rivers with equilibrium banks and mobile bed: 2. The gravel river, *J. Fluid Mech.*, *89*(1), 127–146.

Parker, G., C. Paola, K. X. Whipple, and D. Mohrig (1998), Alluvial fans formed by channelized fluvial and sheet flow: I. Theory, *J. Hydraul. Eng.-ASCE*, *124*(10), 985–995, doi:10.1061/(ASCE)0733-9429(1998)124:10(985.

Roseberry, J. C., M. W. Schmeeckle, and D. J. Furbish (2012), A Probabilistic description of the bed load sediment flux: 2. Particle activity and motions, *J. Geophys. Res.*, *117*, 21, doi:10.1029/2012JF002353.

Schellekens, J., F. N. Scatena, L. A. Bruijnzeel, A. I. J. M. van Dijk, M. M. A. Groen, and R. J. P. van Hogezand (2004), Stormflow generation in a small rainforest catchment in the Luquillo Experimental Forest, Puerto Rico, *Hydrol. Process.*, *18*(3), 505–530, doi:10.1002/hyp.1335.

Scher, H., and E. W. Montroll (1975), Anomalous transit-time dispersion inamorphous solids, *Phys. Rev. B*, *12*(6), 2455–2477, doi:10.1103/PhysRevB.12.2455.

Weeks, E. R., and H. L. Swinney (1998), Anomalous diffusion resulting from strongly asymmetric random walks, *Phys. Rev. E*, *57*(5), 4915–4920, doi:10.1103/PhysRevE.57.4915.

Weeks, E. R., J. S. Urbach, and H. L. Swinney (1996), Anomalous diffusion in asymmetric random walks with a quasi-geostrophic flow example, *Physica D*, *97*(1–3), 291–310, doi:10.1016/0167-2789(96)00082-6.

Wiberg, P. L., and J. D. Smith (1987), Calculations of the critical shear stress for motion of uniform and heterogeneous sediments, *Water Resour. Res.*, *23*(8), 1471–1480, doi:10.1029/WR023i008p01471.

Wolman, M. G. (1954), A method of sampling coarse river-bed material, *Eos. Trans. AGU*, *35*(6), 951–956.

Zhang, Y., M. M. Meerschaert, and A. I. Packman (2012.), Linking fluvial bed sediment transport across scales, *Geophy. Res. Lett.*, *39*, L20404, doi:10.1029/2012GL053476.